Solar-Terrestrial Physics. 2026, vol. 12, iss. 1, pp. 29–39. DOI: 10.12737/stp-121202605.

DOI: 10.12737/stp-121202605
EDN: LADFQG

Received August 07, 2025
Accepted September 20, 2025

MAGNETOTELLURIC SOUNDING AND ELECTROMAGNETIC DIAGNOSTICS OF THE MAGNETOSPHERE AND LITHOSPHERE: POSSIBILITIES OF COMPLEMENTARITY

V.A. Pilipenko
Schmidt Institute of Physics of the Earth RAS, Moscow, Russia, pilipenko_va@mail.ru

E.N. Fedorov
Schmidt Institute of Physics of the Earth RAS, Moscow, Russia, enfedorov1@yandex.ru

D.V. Zinkin
Schmidt Institute of Physics of the Earth RAS, Moscow, Russia, zinkin.deniz@yandex.ru

Abstract. Observations of ultra-low-frequency (ULF) variations in geomagnetic and electrotelluric fields at a network of ground stations are the experimental basis for several geophysical areas: magnetotelluric sounding (MTS) of the earth's crust; hydromagnetic diagnostics of the near-Earth plasma; electromagnetic monitoring of dynamic processes in the lithosphere. The proposed review will demonstrate the possibilities of mutual influence of these seemingly dissimilar areas. Magnetospheric resonance effects can cause distortions of the MTS curve over low-conductive layers near the local resonance frequency, which can be misinterpreted as a feature of the earth's crust structure. On the other hand, a new method of hydromagnetic diagnostics may be adopted that uses both magnetic and electric components of ULF field variations, which can determine the latitudinal variation of the resonance frequency based on data from one observation site. When searching for electromagnetic precursors of earthquakes, we can take an opportunity to separate magnetospheric and seismogenic disturbances, relying on the fact that for ionospheric sources the apparent impedance coincides with the surface impedance of the earth, but the impedance of disturbances created by a lithospheric source exceeds it by an order of magnitude. The question about the presence of an electric mode in the field of geomagnetic pulsations incident on the earth's surface, which is important for MTS sounding, is still controversial. The model of interaction between the Alfvén wave and the ionosphere developed in physics of MHD waves shows a weak excitation of the electric mode. The generation of artificial ULF signals by power lines as a horizontal radiating mega-antenna makes it possible to conduct MTS over a large area.

Keywords: ULF waves, magnetotelluric sounding, magnetosphere diagnostics, electromagnetic earthquake forecasting, active experiments.

INTRODUCTION

Observations of ultra-low-frequency (ULF) variations in the range from a few hertz to the first millihertz of geomagnetic and electrotelluric fields at a network of ground stations are the experimental basis for several research areas in geophysics:

- magnetotelluric sounding (MTS) of conductivity of surface layers of the earth's crust [Kaufman, Keller, 1981];
- hydromagnetic diagnostics of near-Earth plasma based on spectral features of ULF waves [Menk, Waters, 2013];
- electromagnetic monitoring of dynamic processes near earthquake foci [Hayakawa et al., 2007].

These research areas are virtually unrelated, and experts in these areas scarcely cooperate with each other. The proposed review discusses the possibilities of mutual influence of these areas and how these seemingly disparate approaches can be useful to each other. In Introduction, we briefly outline the range of the problems considered.

Existing magnetotelluric models ignore resonance features of ULF wave field spatial structure, determined by MHD wave transformation in the magnetosphere, and assume that the field of geomagnetic pulsations is homogeneous, at least on skin-length scales (the plane wave model) [Vanyan, Butkovskaya, 1980]. As a result, the features governed by resonance effects can be misinterpreted as certain structures in the earth's crust [Pilipenko, Fedorov, 1993].

The theoretical model of resonant transformation of extra-magnetospheric MHD disturbances into Alfvén oscillations of magnetic field lines in the inner magnetosphere predicts the singular behavior of the wave field near a resonance magnetic shell [Kivelson, Southwood, 1986]. Thus, the spectral composition of ULF signals should strongly depend on plasma distribution in the magnetosphere, which allows us to use ground-based observations of ULF pulsations for hydromagnetic diagnosis of near-Earth plasma [Pilipenko et al., 2024a]. For correct hydromagnetic diagnostics, mutually complementary methods are needed to quickly determine the distribution of resonance frequencies in a given region. The main problem with their experimental determination is that the contributions of ULF pulsations from the resonance magnetospheric response and from the oscillation source to the spectral composition are comparable (Figure 1). The observed spectral peak does

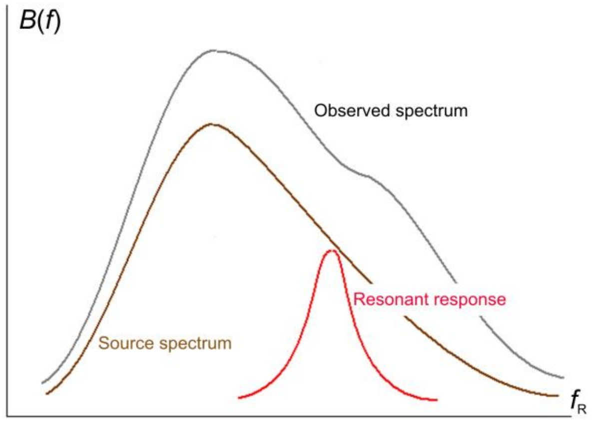

Figure 1. Qualitative representation of the ULF field spectrum as a combination of the source spectrum and the magnetospheric resonance response. The source signal is associated with a disturbance carried by a large-scale magnetosonic wave, and the magnetospheric resonance response at f_R is evoked by the localized response of resonant Alfvén oscillations

not, therefore, necessarily correspond to the local resonance frequency, and the spectral peak width cannot be directly used to define the magnetospheric resonator Q factor. This ambiguity was resolved by the gradient method, in which small-base measurements of spectral amplitude and phase gradients can exclude the influence of the source spectrum shape and identify even relatively weak resonance effects [Baransky et al., 1985]. The local resonance frequency, i.e. eigenfrequency of Alfvén oscillations of magnetic field lines, can be singled out even with unknown parameters of the pulsation source [Pilipenko et al., 1988]. The gradient method [Kurchashov et al., 1987] and its modifications [Guglielmi, 1992] can estimate the field line resonance frequency between stations and the resonance peak width. Despite the apparent simplicity of the one-dimensional model of MHD wave transformation in the magnetosphere [Southwood, 1974], the theoretically predicted amplitude-phase meridional structure corresponds closely to the observed local structure of ULF waves. The region of occurrence of field-line resonances extends from subauroral latitudes to fairly low latitudes [Green et al., 1993]. Different sensitivity of various ULF field components to the magnetospheric field-line resonance suggests that a resonance frequency can be derived not only from the spatial structure, but also from its polarization properties [Baransky et al., 1990; Vellante et al., 1993]. The magnetospheric resonance response is characterized by a pronounced asymmetry of the horizontal components B_x and B_y such that the ratio $|B_x(f)/B_y(f)|$ stands for a maximum at the resonance frequency. It turned out that the phase-amplitude relationships between magnetic and electric components of geomagnetic pulsations can be used to develop a new method for diagnosing Alfvén frequencies (i.e., in fact the magnetospheric plasma density) at a given latitude [Guglielmi, 1989a].

One of the urgent problems of modern geophysics is to lay down physical principles of real-time earthquake prediction based on anomalous disturbances of electromagnetic fields. Monitoring of broadband ULF radiation and pulses, whose sources may be dynamic processes in earthquake foci, seems promising [Guglielmi, Levshenko, 1994; Freund et al., 2021]. Large-scale current systems can form during mountain matter movements along faults upon activation of seismic activity [Gokhberg et al., 1985]. As a result, such movements could be monitored by recording ULF pulses and noise on the earth's surface [Loseva et al., 2010]. Nonetheless, the problem of separating magnetospheric and seismogenic disturbances remains unresolved. The results of calculations of the ULF field on the earth's surface generated by an underground current show its characteristic features in comparison with the field of ionospheric disturbances, which could be used to discriminate endogenous sources [Aleksandrov et al., 2018].

Electromagnetic waves in the atmosphere between the lower ionosphere and the earth's surface can be split into a magnetic H-mode (transverse electric TE) and an electric E-mode (transverse magnetic TH). Each mode has its own partial impedance that characterizes its interaction with the earth's crust. The problem of existence of the E-mode is of key importance for MTS. Considering the incident ULF pulsation field as a superposition of partial E- and H-modes, Chetaev [1985] developed a new MTS method — directional analysis. This method is based on the assumption that the spatial structure of ULF pulsations over a high-resistance crust is inconsistent with the plane-wave approximation and should be modeled as a horizontally propagating inhomogeneous plane wave with a complex wave vector [Chetaev, 1985; Berdichevsky, Dmitriev, 1992]. According to this concept, the E-mode in the atmosphere, which carries a large vertical electric field E_z, is part of the primary wave. In this regard, the possibility of E_z excitation by magnetospheric sources in the atmosphere in the ULF range is critical for applicability of MTS and directional analysis.

Since ULF electromagnetic disturbances are widely used for MTS of the earth's crust, there is an assumption about the possibility of generating artificial signals for this purpose. However, the long-proposed method of exciting Pc1 signals by modulated ionospheric radio heating is very expensive and cannot be implemented without a heating facility. Can a ground-based antenna be employed to excite artificial Pc1 pulsations? However, any noticeable efficiency of ULF-ELF radiation can be expected only for extremely large-scale emitting systems. Such ULF-ELF mega-antennas do exist — this is an extensive global network of power transmission lines (PTLs). PTL disconnected from the main power grid can indeed be utilized as a controlled source of ULF/ELF emissions [Belyaev et al., 2002; Ermakova et al., 2005; Ermakova et al., 2006]. Artificial signals generated by PTL allow MTS to be performed over a vast territory. Such experiments have begun in China to monitor the conductivity of surface layers of the earth's crust by signals from large-scale facilities CSELF (Control Source Extremely Low Frequency) [Zhao et al., 2015] and WEM (Wireless Electromagnetic Method) [Su et al., 2012].

Let us next consider specific examples of the research areas listed above.

1. RESONANCE FEATURES OF THE SPATIAL-FREQUENCY ULF-FIELD STRUCTURE

Studies on physics of ULF waves in near-Earth space have shown that MHD disturbances from remote parts of the magnetosphere (for example, solar wind disturbances, surface waves at the magnetopause, magnetosheath turbulence, etc.) propagate into the magnetosphere and, through mode transformation, excite standing Alfvén oscillations of magnetic field lines. In fact, a giant natural MHD maser operates in the magnetosphere, which is pumped by extra-magnetospheric disturbances, and resonantly generates narrow-band Alfvén waves at the output. These waves passing through the MHD maser's translucent "mirrors" — conjugate ionospheres — in most cases are the sources of quasi-monochromatic Pc3-5 geomagnetic pulsations observed on Earth. Mode transformation is most effective near resonance geomagnetic shells, where the local eigenfrequency $f_R(x)$ of Alfvén field line oscillations coincides with the frequency f of the external source. According to the qualitative theory of differential equations, the mathematical description of the spatial structure of the field disturbance in the magnetosphere near resonance shells can be expressed as an asymptotic expansion in the parameter $x-x_R(f)+i\delta_m$, where x is the magnetic shell coordinate; $x_R(f)$ is the point of Alfvén resonance at which $f=f_R(x)$; δ_m is the resonance region width above the ionosphere [Krylov et al., 1981]. The main term in the asymptotic expression describing the resonance feature of the azimuth component $B_y(x, f)$ in the magnetosphere can be represented as

$$B_y^{(m)}(x,f)=B_0(f)\frac{i\delta_m}{x-x_R(f)+i\delta_m}. \qquad (1)$$

Due to dissipation, oscillation eigenfrequencies have an imaginary addition $\omega_A=2\pi f_R\to\omega_A-i\gamma$, where $\gamma>0$. The resonance width δ_m is related to the attenuation decrement γ by the ratio $\delta_m=-\gamma(\partial_x\omega_A)^{-1}$, i.e. the sign of δ_m depends on the sign of the Alfvén frequency gradient. Since in the entire magnetosphere (except for the plasmapause) $\partial_x\omega_A<0$, then $\delta_m>0$. Based on (1), the latitudinal structure of the ULF field can be qualitatively represented as a combination of the spectrum of the $B_0(f)$ source and the magnetospheric resonance response (see Figure 1). The source signal is associated with a disturbance carried by a large-scale magnetosonic wave and weakly depends on the x coordinate. The magnetospheric resonance response is highly localized and causes abrupt changes in the amplitude and phase of the azimuth component B_y when crossing the resonance shell. The radial component B_x has a weaker logarithmic singularity, so the resonant behavior of this component is barely perceptible.

When passing through the ionosphere, the spatial structure of ULF waves is distorted. This distortion can be analytically described for an Alfvén wave with spatial structure (1) passing through a “thin” ionosphere over infinitely conducting Earth [Alperovich, Fedorov, 2007]. The thin ionosphere approximation assumes that the vertical scale of the wave is much larger than the thickness of the conducting E layer of the ionosphere (~20 km). In the asymptotic case of azimuthal large-scale waves $k_y\ll k_x$ the theory leads to a simple conclusion: oscillations after passing through the ionosphere retain the same spatial structure due to two factors: a) the polarization ellipse rotates by $\pi/2$: $B_y^{(m)}\Rightarrow B_x$ (NS component near the earth), $B_x^{(m)}\Rightarrow B_y$ (EW component near the earth); b) the resonance peak width on the earth widens compared to the peak width above the ionosphere, $\delta=\delta_m+h$, where h is the height of the conducting E layer of the ionosphere (~100 km).

2. RESONANCE FIELD STRUCTURE AND MTS

The horizontal magnetotelluric field components $\mathbf{E}_t=(E_x, E_y)$ and $\mathbf{B}_t=(B_x, B_y)$ recorded on the earth's surface are related by an impedance condition. The surface impedance Z, in turn, is determined by the distribution of the earth's crust conductivity σ in depth z. The magnetotelluric problem consists in measuring $Z(\omega)$ and reconstructing the dependence $\sigma(z)$ from the parametric dependence of the impedance on frequency ω. The physical basis for MTS is the Tikhonov—Kanyar model that characterizes the electromagnetic ULF field over the horizontally homogeneous earth's crust with an impedance that coincides with the plane vertically incident wave impedance Z_g [Berdichevsky, Dmitriev, 2009]. In this case, the impedance ratio is reduced to an extremely simple form

$$\mathbf{E}_t=-\left(\frac{Z_g}{\mu_0}\right)[\mathbf{n}\times\mathbf{B}_t], \qquad (2)$$

where μ_0 is the magnetic permeability of free space; $\mathbf{n}$ is the downward pointing vector of normal to the earth’s surface. Boundary condition (2) is known in the theory of radio wave propagation as the strong skin effect approximation. If the field is homogeneous or linear on the horizontal scale that is greater than the depth of the skin layer $\delta_g=\left(2/(\mu_0\omega\sigma)\right)^{1/2}$ (i.e., $k\delta_g\ll 1$, where k is the horizontal wave vector of disturbance), relation (2) can be used. When the condition for applicability of the strong skin effect breaks down, the apparent impedance is defined not only by geoelectric properties of the underlying crust, but also by the spatial structure of the incident ULF wave [Berdichevsky, Dmitriev, 1992]. For the resonance structure of pulsations, the validity of the strong skin effect approximation reduces to the inequality

$$|k_g\delta|\gg 1,$$

where $k_g=(i\mu_0\sigma\omega)^{1/2}=(1+i)\delta_g^{-1}$ is the wave vector in the earth's crust.

To illustrate the possible distortion of the incident wave field structure under different geoelectric conditions, we present the results of modeling based on analytical results of the passage of a plane incident Alfvén wave through the thin ionosphere [Pilipenko, Fedorov, 1993]. Spatial structure of incident wave (1) is split into spectral harmonics $B(k_x, k_y)$ with spatial parameters k_x, k_y. The impedance condition for individual harmonic of wave on the Earth surface is analytically calculated from the recurrent formula for N homogeneous layers [Wait, 1982]. The total fields $\mathbf{B}(x,y)$ and $\mathbf{E}(x, y)$ are obtained by integrating contributions of all harmonics. For daytime conditions, the selected integral ionospheric Pedersen and Hall conductivities are Σ_P=10 ohm, Σ_H=15 ohm. For the typical Alfvén velocity in the magnetosphere V_A=800 km/s, the wave conductivity of the magnetosphere $\Sigma_A = (\mu_0 V_A)^{-1} = 1$ is much lower than that of the ionosphere. It is assumed that the height of the thin ionosphere h=100 km, the resonance width above the ionosphere δ_m=50 km, and the oscillation period T=100 s.

As a starting point, let us examine the multicomponent amplitude-phase field structure at midlatitudes (geomagnetic latitude Φ ρ=55°) in the vicinity of resonance over the well-conducting earth with a resistivity of 10 ohm ·m (Figure 2, *a*). The horizontal components B_x and E_y have a local maximum at the resonance point (x=0). When moving along the meridian from x=500 km to x=–500 km, B_x and E_y experience a phase jump slightly smaller than π. Near the resonance point x=0, the vertical magnetic component B_z has a gradient twice as steep as B_x. The phase shift between B_z and E_y varies from ~π/2 to ~ –π/2 on different sides of the resonance peak, and at the resonance point these components are in phase. Over a low-resistance medium, the amplitude-phase relations between E_y and B_x are in agreement with the theoretical expression for the plane wave impedance over a homogeneous half-space $Z_g = \sqrt{-i\omega\mu_0/\sigma_g}$ or $|Z_g|^2 = \omega\mu_0\rho$ (Figure 3, *a*).

Let us next analyze distortions of the wave structure over a high-resistance ground (ρ=10^4 ohm·m), where the strong skin effect condition is violated (see Figure 2, *b*) because $|k_g\delta|$~0.4. In this case, the vertical magnetic component becomes comparable to the horizontal one, B_z~B_x. The meridional distribution of amplitudes and phases is distorted, and this distortion is different for the magnetic and electric components. Distortions of the amplitude-phase profiles of B_x and E_y lead to distortion of the apparent impedance profile $Z(x)=\mu_0\, E_y(x)/B_x(x)$. Over a high-resistance medium, distortion of amplitude and phase Z reaches 50 % of the impedance Z_g=2.8 10^{-2} ohm (see Figure 3, *b*). Thus, magnetospheric resonance effects can cause distortions of the standard MTS curve near the local resonance frequency, which can be misinterpreted as a feature of the earth's crust structure [Pilipenko et al., 1998].

Distortion of MTS curves by resonance effects is especially noticeable over weakly conductive layers. An MTS curve $\rho(T)$ for a 4-layer section at 60° latitude from [Alperovich et al., 1991] is exemplified in Figure 4. The section parameters resistance [ohm·m] / power [km] are as follows: 30/3, 3·10^3/50, 3·10^2/50, 3·10^{-2}/∞. The resonance wave structure with T=100 s has a half-width above the ionosphere δ_m=20 km. The solid line denotes the MTS curve in the plane wave approximation; the dashed line, the MTS curve formed by a resonance wave structure. Deviation of the real curve from the plane wave approximation runs to ~30 %.

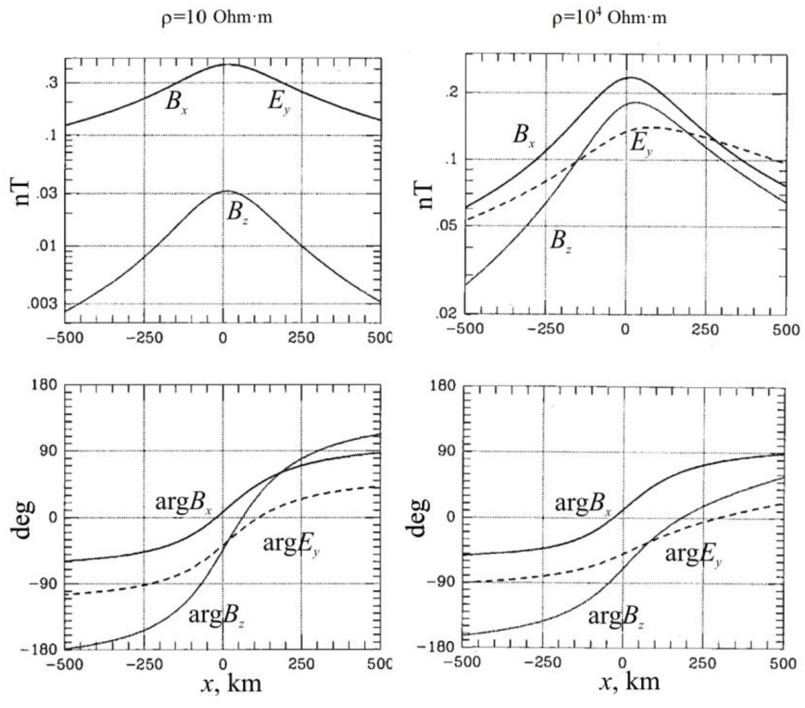

Figure 2. Spatial amplitude-phase structure in the meridional direction near the resonance shell $x = 0$ above a highly conductive crust with a resistivity ρ=10 ohm·m (*a*) and above a low-conducting medium with ρ=10^4 ohm·m (*b*). The incident Alfvén wave has an amplitude B_y=1 nT. The electrical component E_y is normalized to Z_g. The corresponding phase structure is shown in the bottom panel

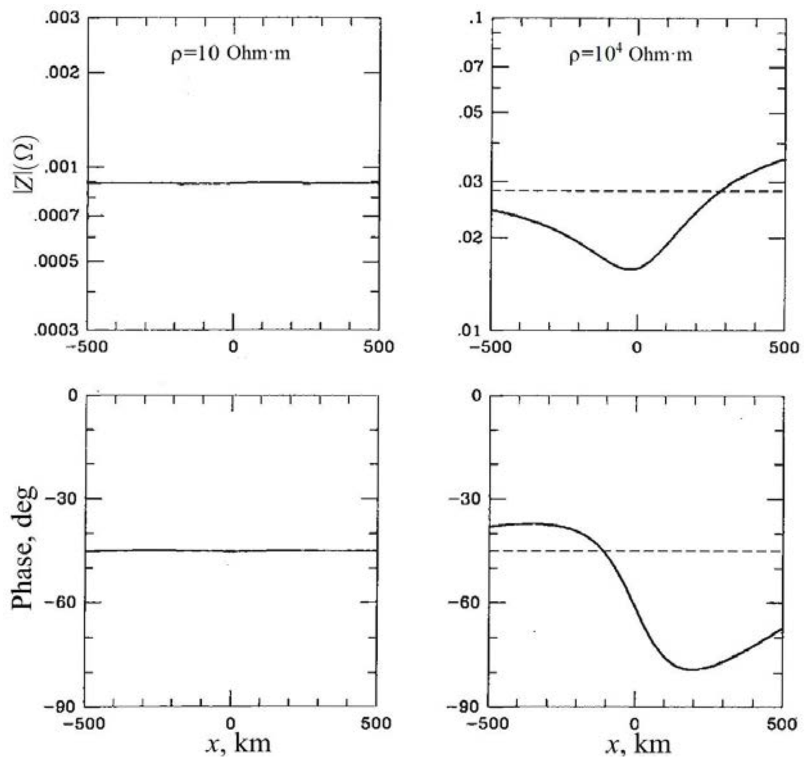

Figure 3. Amplitude (top) and phase (bottom) of apparent impedance Z above a high-conducting earth with ρ=10 ohm·m (*a*) and a low-conducting earth with $\rho=10^4$ ohm·m (*b*). The horizontal dashed line indicates the ground impedance $Z_g \sim 8.9 \cdot 10^{-4}$ohm and $Z_g \sim 2.8 \cdot 10^{-2}$ohm respectively

The described effects manifested themselves during global MTS of the US territory by more than 1000 temporary stations spaced by 70 km. When analyzing MTS curves, it was found that non-physical "bumps" appeared in a significant number of the obtained curves (>15 %) in the frequency range 10–100 s [Murphy, Egbert, 2018]. These distortions are related to resonance effects in the structure of mid-latitude Pc3-4 pulsations.

3. METHODS OF HYDROMAGNETIC DIAGNOSTICS OF MAGNETOSPHERIC PLASMA FROM MTS DATA

The MTS data including recordings of magnetic and electric ULF field components can be used to apply new methods of hydromagnetic diagnostics of magnetospheric plasma distribution [Guglielmi, 1989b]. Thus, the hydromagnetic diagnostics can be supplemented with telluric electric field data.

The vertical magnetic ULF field component B_z is a sensitive indicator of irregularities of both the field itself and the earth's crust conductivity [Southwood, Hughes, 1978]. Thus, the use of B_z data may be promising for identifying resonance features of the spatial structure of geomagnetic pulsations [Green et al., 1991]. The ratio between the vertical and horizontal magnetic ULF field components can be estimated for a strong skin effect from the relation [Wait, 1982]

$$B_z = i(\mu_0\omega)^{-1}\left(Z_g \mathrm{div}\mathbf{B}_t + \mathbf{B}_t \nabla Z_g\right), \quad (3)$$

where div is a 2D divergence operator in the horizontal

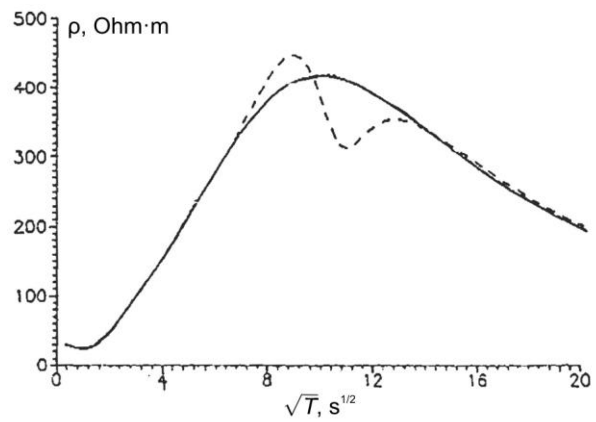

Figure 4. MTS curve $\rho\left(\sqrt{T}\right)$ for a 4-layer section calculated for an incident Alfvén wave with a resonance spatial structure with T=100 s and δ_m=20 km

plane. For Pc3-5 pulsations in regions with horizontally homogeneous crustal conductivity, the meridional gradient $\partial B_x / \partial x$ is the dominant term on the right side of (3). From resonance structure form (1), we obtain

$$B_z = -\frac{Z_g}{\mu_0\omega\delta}\frac{B_x}{1-i\xi}, \quad (4)$$

where $\xi = \left[x - x_R\left(f\right)\right]/\delta$. As follows from (4), the resonance effects in the behavior of B_z may be even more pronounced than in B_x. The complex value of the surface impedance Z_g in (4) can be excluded from consideration through impedance ratio (2). Then the relationship between B_z and E_y reads

$$\frac{B_z}{E_y} = \frac{1}{\omega\delta(1-i\xi)} \quad (5)$$

At the field-line resonance frequency (ξ=0), the ratio between spectral power densities $|B_z(f)/E_y(f)|$ should have a local maximum, and B_z and E_y on their own should be in phase. This analytical estimate is confirmed by the numerical model (Figure 5).

On the basis of the properties of the ULF-field vertical magnetic and horizontal electric components, an additional method of hydromagnetic diagnostics of the magnetosphere can be proposed. It can reconstruct the functional dependence $f_R(x)$ in the vicinity of the observation point, using data from one station [Guglielmi et al., 1989]. The distance between the observation point x and the resonance shell $x_R(f)$, as well as the resonance width δ can be found from (5) as

$$x - x_R = -\omega^{-1}\left|E_y / B_z\right|\sin\psi, \quad \delta = \omega^{-1}\left|E_y / B_z\right|\cos\psi, \quad (6)$$

where $\psi = \arg E_y - \arg B_z$ is the phase difference between the components. Relations (6) allow us to employ multicomponent data from one station to find the distance to the resonance field line at a given frequency. By changing $x_R(f) \Leftrightarrow f_R(x)$ to the inverse relationship, we can determine the latitude dependence of the resonance frequency $f_R(x)$ in the vicinity of the observation point.

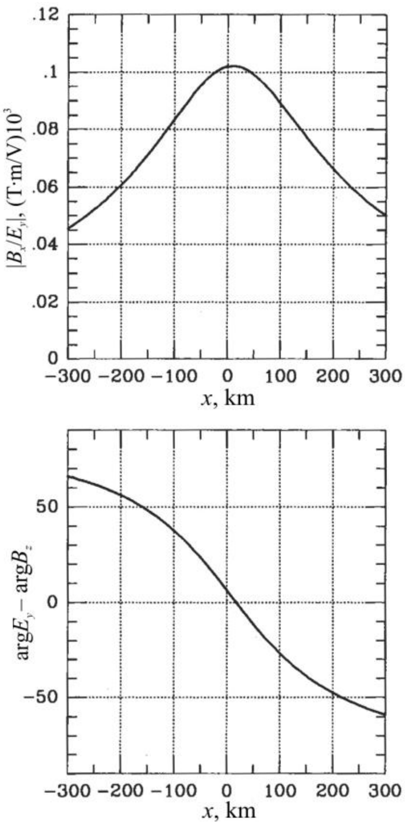

Figure 5. Ratio between B_z and E_y amplitudes at different distances from the resonance field line (*a*) and the phase shift between them (*b*) over the earth's crust with resistivity ρ=10 ohm·m

4. SEARCH FOR RADIATION FROM MOUNTAIN MATTER WITH MTS METHODS

Interest in studying anomalous ULF signals presumably related to earthquakes does not wane. The amplitude of possible electromagnetic disturbances caused by seismic activity is apt to be low. Therefore, to reliably discriminate between seismogenic disturbances it is necessary to develop ad hoc methods of collecting and analyzing data. To identify the characteristic features of seismic anomalous signals, it is necessary to simulate the spatial structure of the field on the earth's surface produced by an underground source. A model has been developed that can numerically calculate ULF fields from underground linear current of finite length in the entire Earth—atmosphere system [Pilipenko et al., 2024c]. The model is based on the mathematical formalism developed by Fedorov et al. [2022] for horizontally stratified media. Mechanical and electrical transformations in the earth's crust generate along a fault an alternating linear current J_o of finite length L, located at a depth $z=-h$ (Figure 6). The source current is closed by conduction currents in the earth's crust and partially penetrates into the atmosphere. This system of oscillating currents creates an electromagnetic field in the atmosphere and earth's crust, which is determined by the numerical model.

Calculation of the spatial field structure shows a parameter that can be used to separate magnetospheric and seismogenic disturbances according to combined electric and magnetic data — the ratio of the apparent impedance (the ratio between spectral amplitudes of horizontal electric and magnetic components $\mu_o|E|/|B|$) to the earth surface impedance Z_g [Mazur et al., 2024]. The apparent impedance of seismogenic disturbances at a frequency of 0.1 Hz, calculated from model values of the magnetic and electrotelluric fields $Z_{xy}=\mu E_x/B_y$, is depicted in Figure 7.

For magnetospheric-ionospheric sources, the apparent impedance of the recorded disturbances for all real conditions coincides with Z_g. On the contrary, for an underground source the ground response impedance is almost an order of magnitude higher than the ground impedance. Thus, monitoring instantaneous impedance

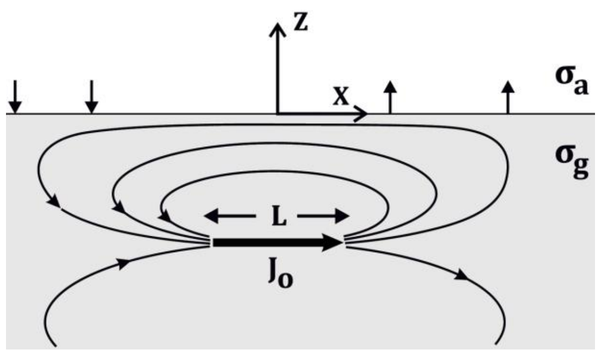

Figure 6. Model of oscillating linear current of length L located at a depth $z=-h$ under the ground and directed along the x axis. Mechanical and electrical transformations in the earth's crust generate a given current J_0, which is then closed by conduction currents in the earth's crust and partially penetrates into the atmosphere

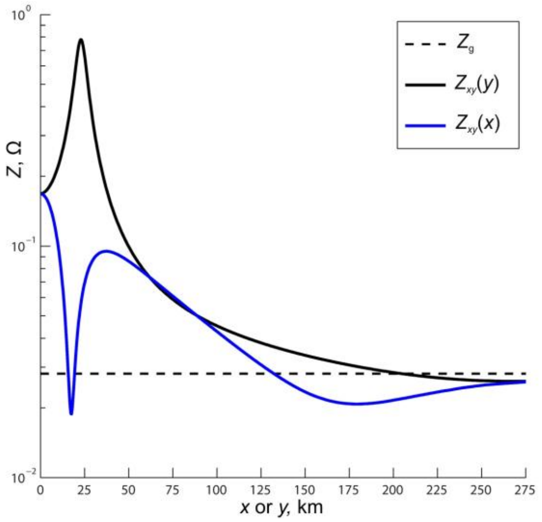

Figure 7. Apparent impedance of seismogenic disturbances $Z_{xy}=\mu_0 E_x/B_y$ at a frequency of 0.1 Hz, calculated from model values of magnetic and electrotelluric fields along (blue curve) and across (black curve) the current J_0

of disturbances during synchronous electrotelluric and geomagnetic observations would make it possible to effectively identify disturbances from seismogenic sources.

5. ELECTRIC MODE OF GEOMAGNETIC PULSATIONS AND MTS

Numerous attempts to detect synchronous ULF pulsations of the geomagnetic field and the atmospheric electric field E_z have yielded contradictory results. On the one hand, multicomponent magnetic and telluric observations have given seemingly promising results confirming the existence of the E-mode [Savin, Israelsky, 2016]. The conclusion about the occurrence of large E_z in the electric mode was presented in [Zybin et al., 1974] as a natural consequence of horizontal propagation of electromagnetic modes in the Earth—ionosphere waveguide. The ULF field in the atmosphere can be locally approximated as an inhomogeneous plane wave with a horizontal wave vector **k**. In this approximation, the vertical component E_z should appear which is related to the magnitude of the horizontal magnetic component $B_\perp$ as follows: $E_z=k/(\omega e_0)B_\perp$. For the commonly observed horizontal phase velocity of Pc3-5 pulsations ω/k~20 km/s, pulsations with an amplitude of $B_\perp$=1 nT have to carry a disturbance E_z~60 V/m. Six-component measurements in a well on low-resistance rocks (ρ=10÷100 ohm·m) confidently recorded E_z~0.01 μV/m in the field of Pc3 pulsations (10–100 s) [Savin et al., 1991]. Measurements with the same equipment over rocks composed of a system of vertical conductive cavities (dikes) yielded, on average, an abnormally large value of E_z~1μ V/m with horizontal components H_x~$5\cdot10^2$μA/m and E_y~0.7 μV/m. The component E_z in the air was estimated from the vertical current continuity J_z at the crust—air interface. $E_z^{(\mathrm{air})}=(\sigma_g/\omega\varepsilon_0)E_z^{(\mathrm{ground})}$. According to this estimate, there should be several tens of V/m for σ_g~10^{-4} S/m and ω~0.01 s^{-1} E_z in the air. However, these studies rely on measurements of the vertical telluric field in wells. It is, therefore, unclear whether the response in E_z to geomagnetic pulsations was actually caused by the incident E-mode or occurred in the earth's crust due to conduction irregularities.

On the other hand, Anisimov et al. [1993] did not find systematic pulsations in the atmospheric field E_z coherent with Pc3 geomagnetic pulsations at midlatitudes. While no agreement between waveforms was observed in the experiment [Bandilet et al., 1980], the events with simultaneous activation of variations in E_z~10 V/m and geomagnetic pulsations and a common spectral composition were interpreted as the excitation of E_z pulsations by a magnetospheric source. Rare events with quasi-periodic variations in E_z might have resulted from wind transport of spatially inhomogeneous aeroelectric structures.

A convincing answer to the question about efficiency of excitation of the electric mode by magnetospheric sources could be obtained in physics of MHD waves in cosmic plasma, which treats of the problem of the interaction between Alfvén waves and the multilayer ionosphere—atmosphere—Earth system [Alperovich, Fedorov, 2007]. Based on this theory, Pilipenko et al. [2021] have developed a numerical model of electromagnetic ULF response to an Alfvén disturbance from the magnetosphere. The model numerically solves a system of coupled wave equations for the realistic ionosphere and atmosphere and allows us to quantify the magnitude of the E_z field that can be expected for geomagnetic disturbances of different types. The geomagnetic field $\mathbf{B}_0$ at high latitudes can be considered vertical. Since the problem is azimuthally symmetric, a cylindrical coordinate system {z, ρϕ} with ρ=0 on the current tube axis is applied. The impedance boundary condition $E_\phi/B_\rho=E_\rho/B_\phi=Z_g/\mu_0$ is imposed on the atmosphere—Earth boundary. The ionospheric collisional plasma parameters were reconstructed using IRI [http://irimodel.org]. The IRI parameters were chosen to correspond to midnight at the auroral latitude. The vertical profile of atmospheric conductivity is modeled by the exponential dependence $\sigma_A(z)=\sigma_0\exp(z/\alpha)$, which is joined with the conductivity from IRI for z=80 km; surface conductivity $\sigma_0=10^{-14}$ S/m. The complex atmospheric conductivity including the displacement current is defined by the expression $\sigma(z)=\sigma_A(z)-i\varepsilon_0\omega$, where ε_0 is the permittivity of free space. Obviously, at low altitudes σ(z) depends on the displacement current; and at high altitudes, on the conduction current. We calculated the horizontal distribution of six electromagnetic field components, including the vertical electric field in the atmosphere excited by an incident Alfvén wave.

The magnetic mode in the atmosphere is excited by ionospheric Hall currents. These eddy currents cause a magnetic response in the radial direction, i.e. in B_ρ. The electric mode in the atmosphere is associated with the vertical current that generates a magnetic disturbance in B_ϕ. Thus, B_ρ and E_ϕ are associated with the H-mode; and B_ϕ and E_ρ, with the E-mode. The vertical electric component E_z related to the E-mode has a maximum under the source at ρ=0 (Figure 8). At distances to ~10^3 km, E_e decreases very slowly, but drops sharply at distances >10^3 km. For a lower frequency, the drop begins earlier.

Numerical simulations have shown that the excitation of the E-mode by magnetospheric sources is very weak and this mode practically does not contribute to the magnetic field of ULF pulsations on the Earth surface. The contribution of the E-mode to the horizontal telluric field induced by ULF pulsations is also insignificant. Under most favorable conditions, a large-scale intense (~100 nT) geomagnetic disturbance could cause only a weak E_z disturbance of the order of several V/m. Therefore, the assumption of the directional analysis [Chetaev, 1985; Zybin et al., 1974; Savin, Israelsky, 2016] about the occurrence of the E-mode in the field of incident ULF waves is not supported by the concepts of magnetospheric sources of geomagnetic pulsations. The mathematical formalism developed in the directional analysis can nonetheless be applied to VLF MTS (for example, Schumann resonance) or to MTS with artificial signals from mega-antennas.

6. MTS WITH ARTIFICIAL ULF SIGNALS

ULF waves in the hertz frequency range (Pc1 pulsations) are of particular importance for space physics. Due to the resonant wave—particle interaction, Pc1 electromagnetic ion-cyclotron waves can cause relativistic electron precipitation from the outer radiation belt into the atmosphere and thus reduce killer electron fluxes to a safe level for satellite electronics. Therefore, the idea even arose in space physics to artificially excite Pc1 electromagnetic waves by modulated ionospheric radio heating [Guo et al., 2021]. In early experiments with the SURA facility on modulated heating of the dayside ionosphere, it was possible to detect the excitation of magnetic pulsations at a modulation frequency of 3 Hz with an amplitude of the order of several nanotesla 100 km from the transmitter

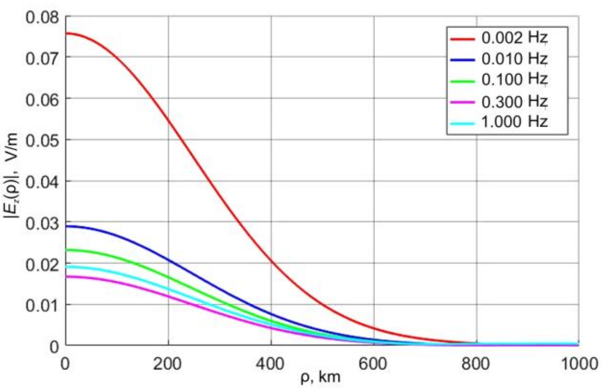

Figure 8. Horizontal distribution of the vertical electric field E_z(ρ) in the atmosphere, which is excited by an incident Alfvén wave with different frequencies. Amplitudes of all components are normalized so that to obtain a single magnetic disturbance on Earth $B_\rho(z=0)$=1 nT in the region of the spatial maximum ρ=ρ_{max}. Homogeneous ground conductivity is taken to be $\sigma_g=10^{-4}$ S/m

[Getmantsev et al., 1977]. Heating of the E-layer presumably leads to variations in the electron collision frequency on which the ionospheric collisional plasma conductivity depends, so that periodic modulation of the ionospheric current exciting geomagnetic pulsations occurs in the heating region. Modulated heating of the F-region can also generate ionospheric currents, which act as an antenna for injecting Pc1 waves into the ionospheric waveguide. The wave response at the modulation frequency of the F layer was detected by ground-based magnetometers in the vicinity of the heating facility [Eliasson et al., 2012; Kotik et al., 2013]. Excited artificial signals with a given frequency could be used for MTS of the earth's crust in the region of heating facility operation. There is, however, a more efficient and much cheaper method of exciting artificial ULF signals, which can be implemented in almost any region.

FENICS (Fennoscandian Electrical conductivity from soundings with the Natural and Controlled Sources) experiments are conducted on the Kola Peninsula with controlled sources of ULF/ELF electromagnetic fields, utilizing PTL as a horizontal radiating antenna [Velikhov et al., 1994; Zhamaletdinov et al., 2015]. The main objectives of the experiments are to examine the propagation features of ULF-ELF electromagnetic signals in the Earth—ionosphere waveguide. From July 25 to August 8, 2024, the next FENICS-2024 experiment was performed in two stages [Pilipenko et al., 2025].

- At the first stage, the Vykhodnoy—Olenegorsk (VKH—OLE) PTL 95.6 km long and with a distance between groundings of the substations L=84 km was employed.
- At the second stage, the Vykhodnoy—Nickel (VKH—NIK) PTL of length 205 km and with L=130 km was used.

During the experiment, a 200 kW generator in PTL produced an alternating current ~140–150 A at low frequencies (1–10 Hz) to ~40 A at the highest frequencies (194 Hz), which was applied at night according to a schedule of 15 min sessions. The temporary shutdown of one line did not affect the electric power supply to consumers, as electricity was transmitted through the remaining sections of the main power grid.

To study the propagation features of ULF signals, the horizontal magnetic field components were observed at several magnetic stations with highly sensitive equipment (Figure 9):

- the Radio Astronomy Observatory Staraya Pustyn (PUS) at R~1560 km away from VKH;
- the station Istok (IST) ~100 km north of Norilsk, R~2100 km away from VKH;
- the geophysical station Lovozero (LOZ) at R~185 km away from the center of radiating line;
- the Hydrometeorological Observatory Barentsburg (BRB) at R~1130 km away.

Artificial signals emitted by PTLs at relatively close LOZ and BRB far exceeded the intensity of natural Pc1 pulsations. Even at remote PUS and IST, spectra revealed weak but noticeable peaks corresponding to the occurrence of artificial harmonic emissions in the respective sessions.

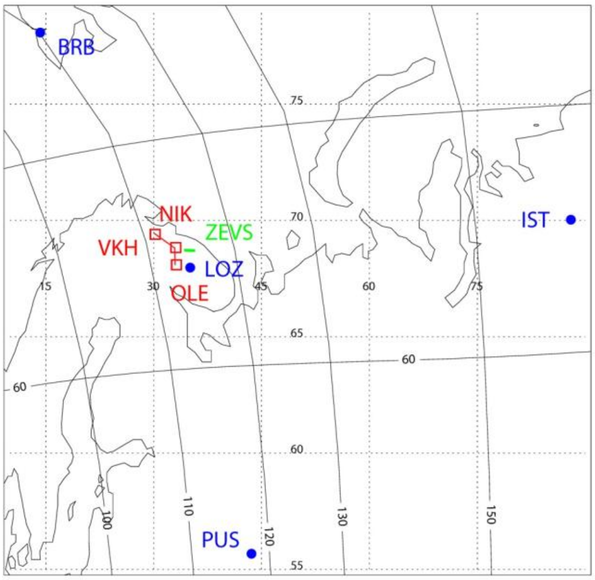

Figure 9. Map of PTL substations (red squares) and magnetic stations (blue dots) (see also [Pilipenko et al., 2025]

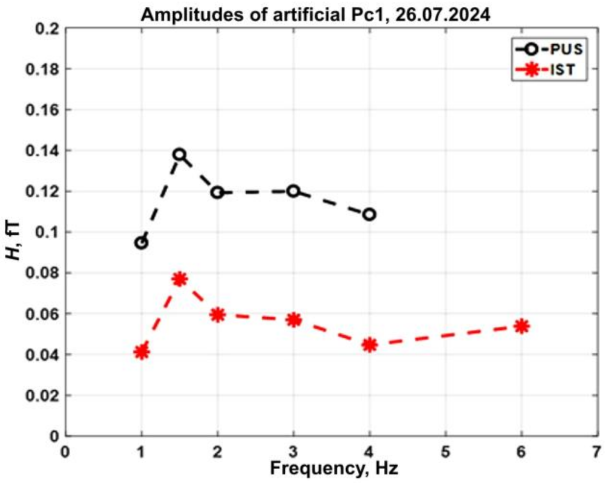

Figure 10. Normalized amplitudes of artificial Pc1 signals (*H* component) at different frequencies at PUS (*R*~1560 km) and IST (*R*~2100 km): 0.6 ±0.2 and 0.3 ±0.05 fT/A

At PUS at 1–4 Hz, the normalized signal amplitudes in all sessions were 0.6±0.2 fT/A. At IST, the normalized amplitudes of recorded signals were 0.3±0.05 fT/A on the average. The amplitude of artificial signals decreased rapidly at a small distance (<300 km) from the emitter, but at large distances the decrease was rather slow. Thus, the amplitudes of artificial Pc1 signals at 1–4 Hz frequencies at *R*~1560 km are, on average, only twice as large as the amplitude at *R*~2100 km (Figure 10).

The FENICS results have shown that PTLs disconnected from the main power grid can be utilized as a controlled source of ULF waves. In the FENICS-2024 experiment, 1–6 Hz artificial signals were detected at a distance >2000 km. Such long-range propagation has never been observed in experiments on ionospheric radio heating. Thus, a FENICS-type heating facility can be a much cheaper and more effective alternative to radio-heating methods for exciting artificial radiation [Pilipenko et al., 2024b], allowing MTS to be performed in almost any region.

Allowance must, however, be made for the difference between artificial signals and natural ULF pulsations. If the natural pulsations excited by ionospheric currents are dominated by the magnetic mode, both magnetic and electric modes contribute to the structure of artificial signals excited by a horizontal antenna. Over high-resistance rocks (such as granites on the Kola Peninsula), surface impedances of these modes differ, and for correct MTS it is necessary to apply the directional analysis method that can distinguish between contributions of electric and magnetic modes [Chetaev, 1985].

CONCLUSION

There are still enormous potentials for mutual enrichment of MTS methods for conductivity of surface layers of the earth's crust and hydromagnetic diagnostics of near-Earth plasma with spectral features of ULF waves. The presence of a resonance structure of the geomagnetic pulsation field leads to a distortion of the MTS curve at resonance frequencies, especially over high-resistance rocks. To estimate the frequencies that are "dangerous" for MTS, it is necessary to predetermine the distribution of resonance frequencies for the region under study, using methods of hydromagnetic diagnostics. On the other hand, an additional method of hydromagnetic diagnostics can be proposed, which employs data from MTS stations. With this method, we can determine the latitude dependence of the resonance frequency in the finite region from data obtained at one point. The MTS methods may be useful in searching for electromagnetic precursors of earthquakes to separate magnetospheric and seismogenic disturbances. Monitoring of the apparent impedance of electromagnetic ULF fields can be used to detect weak seismogenic disturbances. The model of interaction between the Alfvén wave and the ionosphere—ionosphere—Earth system developed in physics of magnetospheric MHD waves helps to solve the problem of the possible contribution of the electric mode that has long been in the MTS theory. The first active experiments with PTL as an emitter of artificial ULF waves open up the possibility of real-time MTS of surface layers of the earth's crust over a huge area. Most of the promising research areas described in the review have not yet been experimentally tested.

The work of D.V. Zinkin was financially supported by RSF (Grant No. 25-47-01004).

REFERENCES

Aleksandrov P.N., Rybin A.K., Zabinyakova O.B. Separation of the electromagnetic field by the position of sources in the magnetotelluric method. *Scientific Notes of Kazan University*. 2018, vol. 160, book 2. pp. 339–351.

Alperovich L.S., Fedorov E.N. Hydromagnetic waves in the magnetosphere and the ionosphere. *Astrophys. Space Sci. Library*. 2007, vol. 353, Springer, Berlin, 418 p.

Alperovich L.S., Fedorov E.N., Osmakova T.B. On the features of the telluric field near the resonant magnetic shell. *Bull. USSR Academy of Sciences, Physics of the Solid Earth*. 1991, iss. 7, pp. 60–71.

Anisimov S.V., Kurneva N.A., Pilipenko V.A. Input of electric mode into the field of Pc3-4 pulsations. *Geomagnetism and Aeronomy*. 1993, vol. 33, iss. 3, pp. 35–41.

Bandilet O.I., Zemlyankin G.I., Fedorenko Yu.V. Pulsations of the vertical component of the geoelectric field in the Pi1-2 and Pc1 ranges. *Geomagnetism and Aeronomy*. 1980, vol. 20, iss. 1, pp. 165−168.

Baransky L.N., Borovkov Yu.E., Gokhberg M.B., et al. High resolution method of direct measurement of the magnetic field line's eigen frequencies. *Planetary and Space Sci*. 1985, vol. 33, iss. 12, pp. 1369–1374. DOI: 10.1016/0032-0633(85)90112-6.

Baransky L.N., Belokris S.P., Borovkov Yu.E., Green C.A. Two simple methods for the determination of the resonance frequencies of magnetic field lines. *Planetary and Space Sci*. 1990, vol. 38, no. 12, pp. 1573–1576. DOI: 10.1016/0032-0633(90)90163-k.

Berdichevsky M.N., Dmitriev V.I. *Magnetotelluric Sounding of Horizontally Homogeneous Media*. Moscow: Nedra, 1992, 250 p. (In Russian).

Berdichevsky M.N., Dmitriev V.I. *Models and Methods of Magnetotellurics*. Moscow: Scientific World, 2009, 680 p. (In Russian).

Belyaev P.P., Ermakova E.N., S.V. Isaev, et al. First experiments on generating and receiving artificial ULF emissions (0.3–12 Hz) at a distance of 1500 km. *Radiophysics and Quantum Electronics*. 2002, vol. 45, iss. 2, pp. 135–146.

Chetaev D.N. *Directional Analysis of Magnetotelluric Observations*. Moscow: IFZ AN SSSR, 1985, 228 p. (In Russian).

Eliasson B., Chang C.-L., Papadopoulos K.J. Generation of ELF and ULF electromagnetic waves by modulated heating of the ionospheric F2 region. *J. Geophys. Res*. 2012, vol. 117, art. no. A10320. DOI: 10.1029/2012JA017935.

Ermakova E.N., Kotik D.S., Sobchakov L.A., et al. Experimental studies of propagation of artificial electromagnetic signals in the range of 0.6–4.2 Hz. *Izvestiya vuzov. Radiofizika [Radiophysics and Quantum Electronics]*. 2005, vol. 48, no. 9, pp. 788–799.

Ermakova E.N., Kotik D.S., Polyakov S.V., et al. A power line as a tunable ULF-wave radiator: Properties of artificial signal at distances of 200 to 1000 km. *J. Geophys. Res.* 2006, vol. 111, A04305. DOI: 10.1029/2005JA011420.

Fedorov E.N., Mazur N.G., Pilipenko V.A. Electromagnetic fields in the upper ionosphere from a horizontal ELF ground-based finite-length emitter. *Izvestiya VUZ Radiofizika*. 2022, vol. 65, no. 9, pp. 697–712. DOI: 10.52452/00213462_2022_65_09_697.

Freund F.T., Heraud J.A., Centa V.A., Scoville J. Mechanism of unipolar electromagnetic pulses emitted from the hypocenters of impending earthquakes. *The European Physical J. Special Topics*. 2021, vol. 230, pp. 47–65. DOI: 10.1140/epjst/e2020-000244-4.

Getmantsev G.G., Guglielmi A.V., Klein B.I., et al. Excitation of magnetic pulsations when the ionosphere is exposed to radiation from a powerful short-wave transmitter. *Izvestiya vuzov. Radiofizika [Radiophysics and Quantum Electronics]*. 1977, vol. 20, no. 7, pp. 1017–1019.

Gokhberg M.B., Gufeld I.L., Gershenzon N.I., Pilipenko V.A. Effects of electromagnetic nature during destruction of the earth's crust. *Izvestiya AN SSSR Physics of the Solid Earth*. 1985, no. 1, pp. 72–87.

Green A.W., Worthington E.W., Pilipenko V.A., et al. Influence of magnetospheric Alfven resonance on the spectrum of Pc3-4 pulsation packets at midlatitudes. *Geomagnetism and Aeronomy*. 1991, vol. 31, iss. 4, pp. 619–624.

Green A.W., Worthington E.W., Baransky L.N., et al. Alfven field line resonances at low latitudes (L=1.5). *J. Geophys. Res.* 1993, vol. 98, pp. 15693–15699. DOI: 10.1029/93ja00644.

Guglielmi A.V. Diagnostics of the plasma in the magnetosphere by means of measurement of spectrum of Alfven oscillations. *Planetary and Space Sci*. 1989a, vol. 37, iss. 8, pp. 1011–012. DOI: 10.1016/0032-0633(89)90055-X.

Guglielmi A.V. Hydromagnetic diagnostics and geoelectric sounding. *Physics-Uspekhi.* 1989b, vol. 32, iss. 8, pp. 678–696. DOI: 10.1070/PU1989v032n08ABEH002747.

Guglielmi A.V. Hydromagnetic diagnostics of the space environment. *Izvestiya AN SSSR Physics of the Solid Earth*. 1992, no. 5, p. 45.

Guglielmi A.V., Levshenko V.T. Electromagnetic signals from earthquakes. *Izvestiya AN SSSR Physics of the Solid Earth*. 1994, no. 5, pp. 65–70.

Guglielmi A.V., Gokhberg M.B., Ruban V.F. Hydromagnetic diagnostics and geoelectric prospecting based on a single observatory. *Rep. USSR Academy of Sciences*. 1989, vol. 308, no. 3, pp. 578–581.

Guo Z., Fang H., Honary F. The generation of ULF/ELF/VLF waves in the ionosphere by modulated heating. *Universe*. 2021, vol. 7, no. 2, p. 29. DOI: 10.3390/universe7020029.

Hayakawa M., Hattori K., Ohta K. Monitoring of ULF geomagnetic variations associated with earthquakes. Sensors. 2007, vol. 7, no. 7, pp. 1108–1122. DOI: 10.3390/s7071108.

Kaufman A.A., Keller G.V. The magnetotelluric sounding method. *Elsevier Science*. 1981, New York, 595 p.

Kivelson M.G., Southwood D.J. Coupling of global magnetospheric MHD eigenmodes to field line resonances. *J. Geophys. Res*. 1986, vol. 91, p. 4345.

Kotik D.S., Ryabov A.V., Ermakova E.N., et al. Properties of ULF/VLF signals generated by the SURA installation in the upper ionosphere. *Izvestiya vuzov. Radiofizika [Radiophysics and Quantum Electronics]*. 2013, vol. 56, iss. 6, pp. 382–394.

Krylov A.L., Lifshits A.E., Fedorov E.N. On the resonance properties of the magnetosphere. *Izvestiya RAS Physics of the Solid Earth*. 1981, iss. 6, p. 49.

Kurchashov Yu.P., Nikomarov Ya.S., Pilipenko V.A., Best A. Local meridional structure of mid-latitude geomagnetic pulsations. *Ann. Geophys.* 1987, vol. 5A, p.147.

Loseva T.V., Kuzmicheva M.Yu., Spivak A.A. Electric and magnetic signals during constrained movements of crustal blocks. *Rep. Russian Academy of Sciences*. 2010, vol. 432, no. 5, pp. 685–688.

Mazur N.G., Fedorov E.N., Pilipenko V.A., Borovleva K.E. Electromagnetic ULF fields on the Earth's surface and in the ionosphere from an underground seismic source. *Izvestiya RAS. Physics of the Solid Earth*. 2024, iss. 2, pp. 59–71. DOI: 10.31857/S0002333724020058.

Menk F.W., Waters C.L. *Magnetoseismology: Ground-based remote sensing of Earth's magnetosphere*. 2013, p. 271.

Murphy B.S., Egbert G.D. Source biases in midlatitude magnetotelluric transfer functions due to Pc3-4 geomagnetic pulsations. *Earth, Planets and Space.* 2018, vol. 70, no. 12. DOI: 10.1186/s40623-018-0781-0.

Pilipenko V.A., Fedorov E.N. Magnetotelluric sounding of the crust and hydromagnetic monitoring of the magnetosphere with the use of ULF waves. *Ann. Geofisic.* 1993, vol. 36, no. 5-6, pp. 19–33.

Pilipenko V.A., Povzner T.A., Savin I.V., Nikomarov Ya.N. Local spatial structure of the geomagnetic pulsation field at midlatitudes. *Izvestiya AN SSSR Physics of the Solid Earth*. 1988, no. 10, pp. 54–61.

Pilipenko V., Vellante M., Anisimov S., et al. Multi-component ground-based observation of ULF waves: goals and methods. *Ann. Geofis*. 1998, vol. 41, no. 1, pp. 63–77.

Pilipenko V.A., Fedorov E.N., Martines-Bedenko V.A., Bering E.A. Electric mode excitation in the atmosphere by magnetospheric impulses and ULF waves. *Frontiers in Earth Science.* 2021, vol. 8, p. 87. DOI: 10.3389/feart.2020.619227.

Pilipenko V.A., Pozdnyakova D.D., Savelyeva N.V. Ultra-low-frequency waves in space and on *Earth. International Journal of Humanities and Natural Sciences*. 2024a, vol.

96, no. 9-3, pp. 163–205. (In Russian). DOI: 10.24412/2500-1000-2024-9-3-163-205.

Pilipenko V.A., Mazur N.G., Fedorov E.N., Shevtsov A.N. On the possibility of experiments on the excitation of artificial ultra-low-frequency radiation in the ionosphere by the FENICS installation on the Kola Peninsula. *Bull. RAS. Phys. Series*. 2024b, vol. 88, iss. 3, pp. 392–400.

Pilipenko V.A., Mazur N.G., Fedorov E.N. Discrimination of ULF signals from an underground seismogenic current. *Earth, Planets and Space*. 2024c, vol. 76, no. 118. DOI: 10.1186/s40623-024-02058-9.

Pilipenko V.A., Ermakova E.N., Potapov A.S., et al. Excitation of global artificial Pc1 signals during FENICS-2024 experiment: 1. Observations. *Sol.-Terr. Phys*. 2025, vol. 11, iss. 2, pp. 111–118. DOI: 10.12737/stp-112202511.

Savin M.G., Nikiforov V.M., Kharitonov V.M. On anomalies of the vertical electric component of the magnetotelluric field in Northern Sakhalin, *Physics of the Solid Earth.* 1991, no. 2, pp. 100–108.

Savin M.G.; Izrailsky Yu.G. New possibilities of the Chetaev model. *Sol.-Terr. Phys*. 2016, vol. 2, iss. 2, pp. pp. 104–114. DOI: 10.12737/21003.

Southwood D.J. Some features of field line resonances in the magnetosphere. *Planetary and Space Sci*. 1974, vol. 22, p. 483.

Southwood D.J., Hughes W.J. Source induced vertical components in geomagnetic pulsation signals. *Planetary and Space Sci.* 1978, vol. 26, pp. 715–720.

Su B., Wang Y., Cao Q. Simulation of WEM using ELF modeling of local area and modified UPML. *ISAPE2012*, 2012, pp. 983–986. DOI: 10.1109/ISAPE.2012.6408939.

Vanyan L.L., Butkovskaya A.I. *Magnetotelluric Sounding of Layered Media*. Moscow: Nedra Publ., 1980. (In Russian).

Velikhov E.P., Zhamaletdinov A.A., Sobchakov L.A., et al. Experience of frequency electromagnetic sounding of the earth's crust using a powerful ULF antenna. *Doklady RAS.* 1994, vol. 338, no. 1, pp. 106–109.

Vellante M., Villante U., De Lauretis M., et al. Simultaneous geomagnetic pulsation observations at two latitudes: resonant mode characteristics. *Ann. Geophys.* 1993, vol. 11, pp. 734–741.

Wait J.R. Geoelectromagnetism. *Academic Press*, 1982.

Zhamaletdinov A.A., Shevtsov A.N., Velikhov E.P., et al. Study of interaction of electromagnetic waves of the ELF-ULF range (0.1–200 Hz) with the earth's crust and ionosphere in the field of industrial power transmission lines (experiment "FENICS"). *Geophysical Processes and Biosphere*. 2015, vol. 14, iss. 2, pp. 5–49.

Zhao G.Z, Bi Y.X., Wang L.F., et al. Advances in alternating electromagnetic field data processing for earthquake monitoring in China. *Science China Earth Sciences.* 2015, vol. 58, no. 2, pp.172–182. DOI: 10.1007/s11430-014-5012-3.

Zybin K.Yu., Krylov S.M., Lependin V.P., et al. On the vertical electrical strength of the field of geomagnetic pulsations. *Proc. Academy of Sciences of USSR.* 1974, vol. 218, iss. 4, pp. 828–829. (In Russian).

URL: http://irimodel.org (accessed May 3, 2025).

Original Russian version: Pilipenko V.A., Fedorov E.N., Zinkin D.V., published in Solnechno-zemnaya fizika. 2026, vol. 12, no. 1, pp. 33–44. DOI: 10.12737/szf-121202605.

How to cite this article

Pilipenko V.A., Fedorov E.N., Zinkin D.V. Magnetotelluric sounding and electromagnetic diagnostics of the magnetosphere and lithosphere: Possibilities of complementarity. *Sol.-Terr. Phys*. 2026, vol. 12, iss. 1, pp. 29–39. DOI: 10.12737/stp-121202605.